# Supporting Information

## Self-supported porous $NiSe_2$ nanowrinkles as efficient bifunctional electrocatalysts for overall water splitting

Jie Zhang,[a] Ying Wang,[a] Chi Zhang,[b] Hui Gao,[a] Lanfen Lv,[a] Lulu Han,[a] Zhonghua Zhang[a,b,*]

[a]Key Laboratory for Liquid-Solid Structural Evolution and Processing of Materials (Ministry of Education), School of Materials Science and Engineering, Shandong University, Jingshi Road 17923, Jinan 250061, P.R. China

[b]School of Applied Physics and Materials, Wuyi University, 22 Dongcheng Village, Jiangmen 529020, PR China

*Corresponding author. Email: zh_zhang@sdu.edu.cn (Z. Zhang).

**This part includes:**

Figures S1- S16

Tables S1-S4

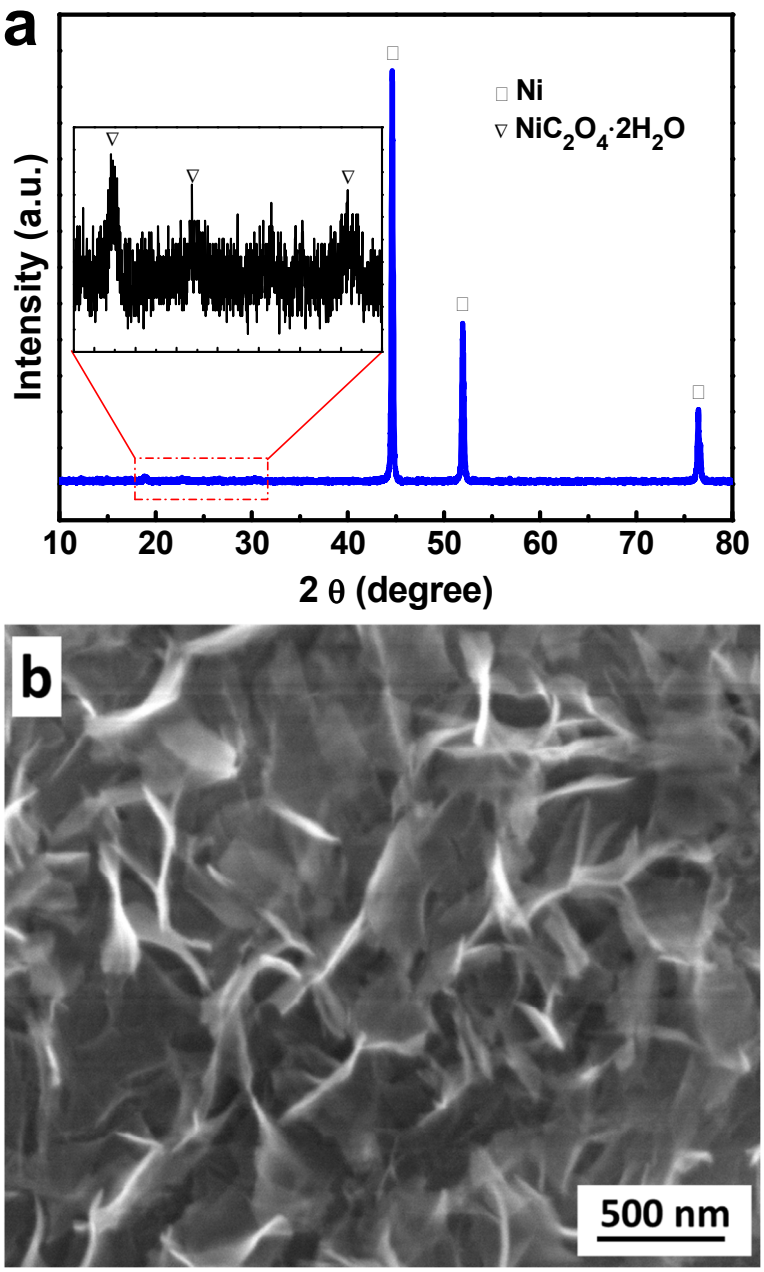


Figure S1. (a) XRD pattern and (b) SEM image of $NiC_2O_4 \cdot 2H_2O$.

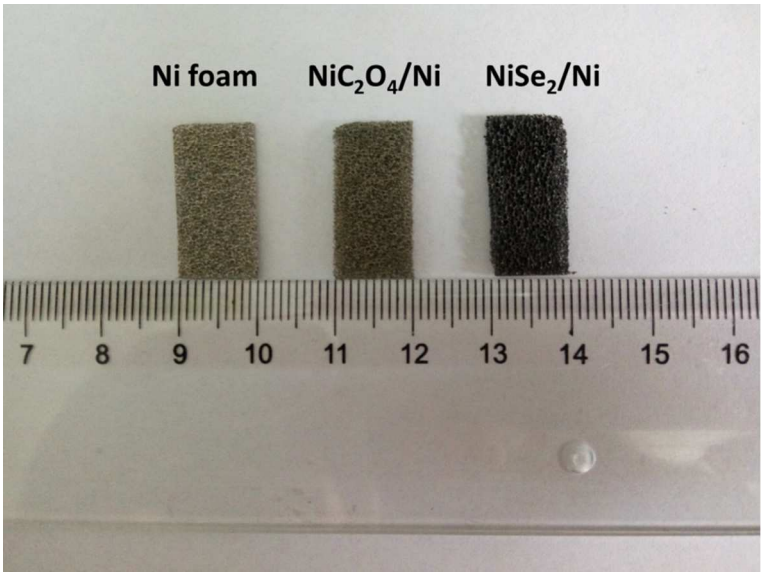


Figure S2. Optical photographs of Ni foam, $NiC_2O_4$/Ni and $NiSe_2$/Ni.

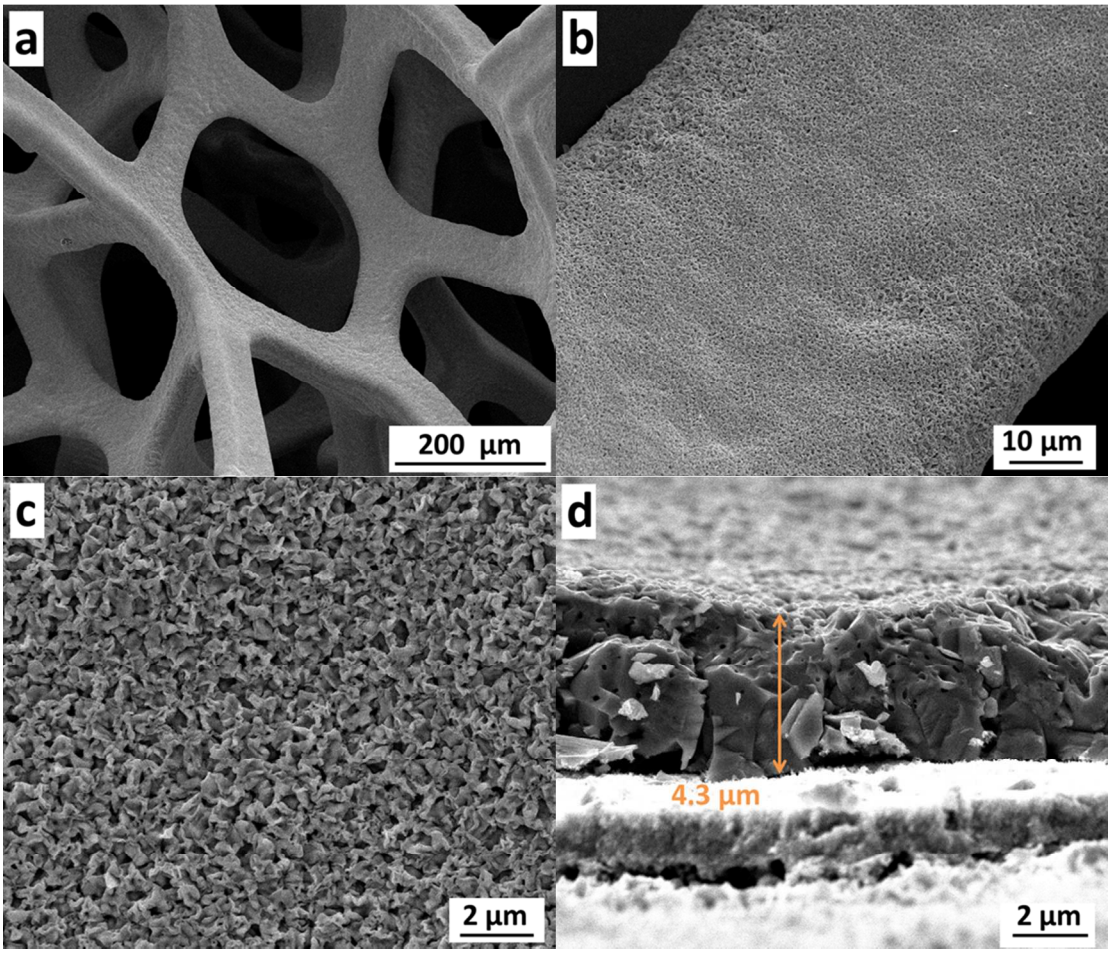


Figure S3. Top-view SEM images (a, b and c) showing the morphology of the $NiSe_2$ nanowrinkles anchored on Ni foam at different magnifications. (d) Cross-view SEM image showing the thickness of $NiSe_2$ layer on the skeleton surface.

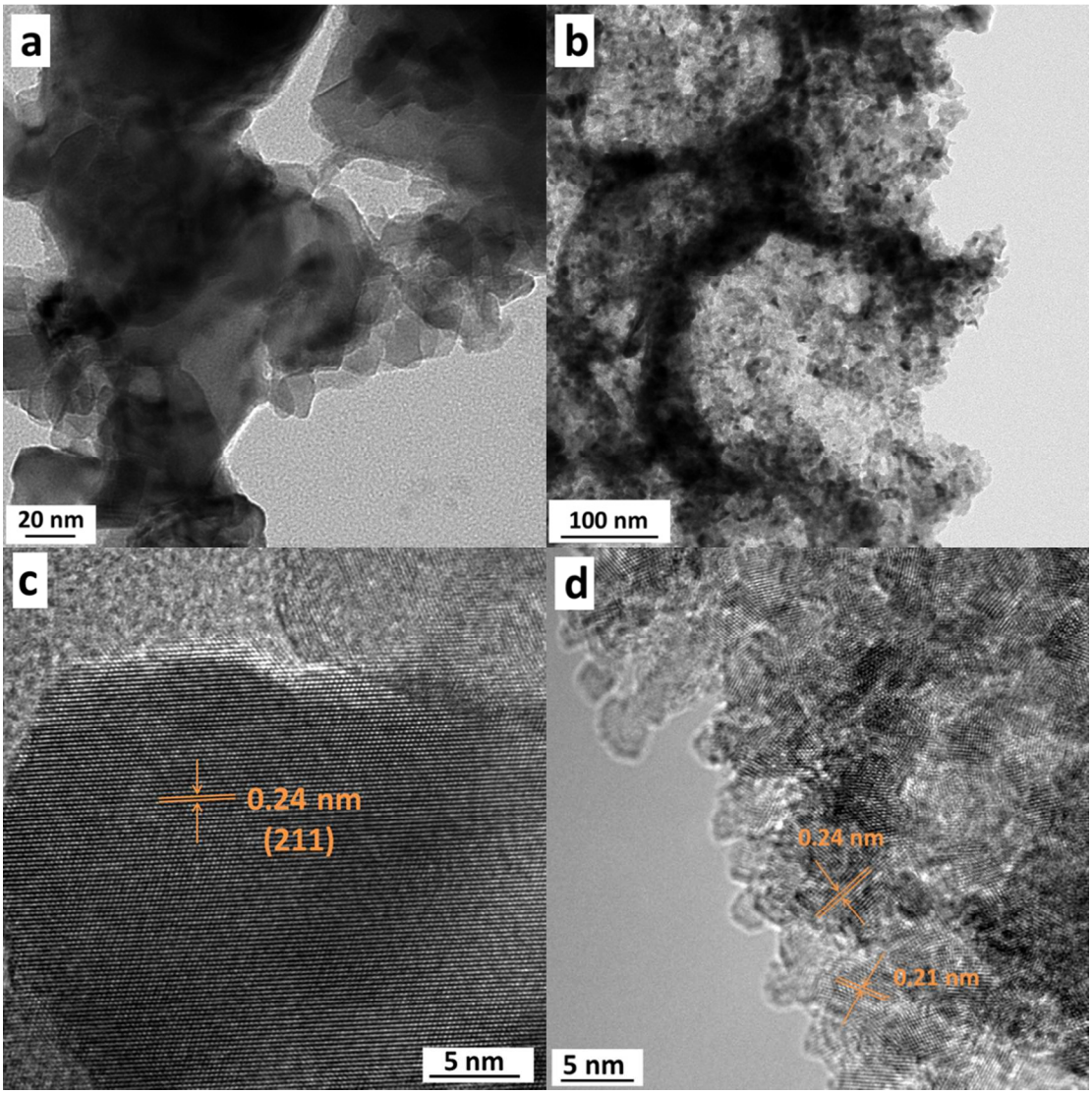


Figure S4. TEM images (a and b) showing the $NiSe_2$ layer with porous nanowrinkle structure. The HRTEM images (c and d) showing the lattice fringes of $NiSe_2$.

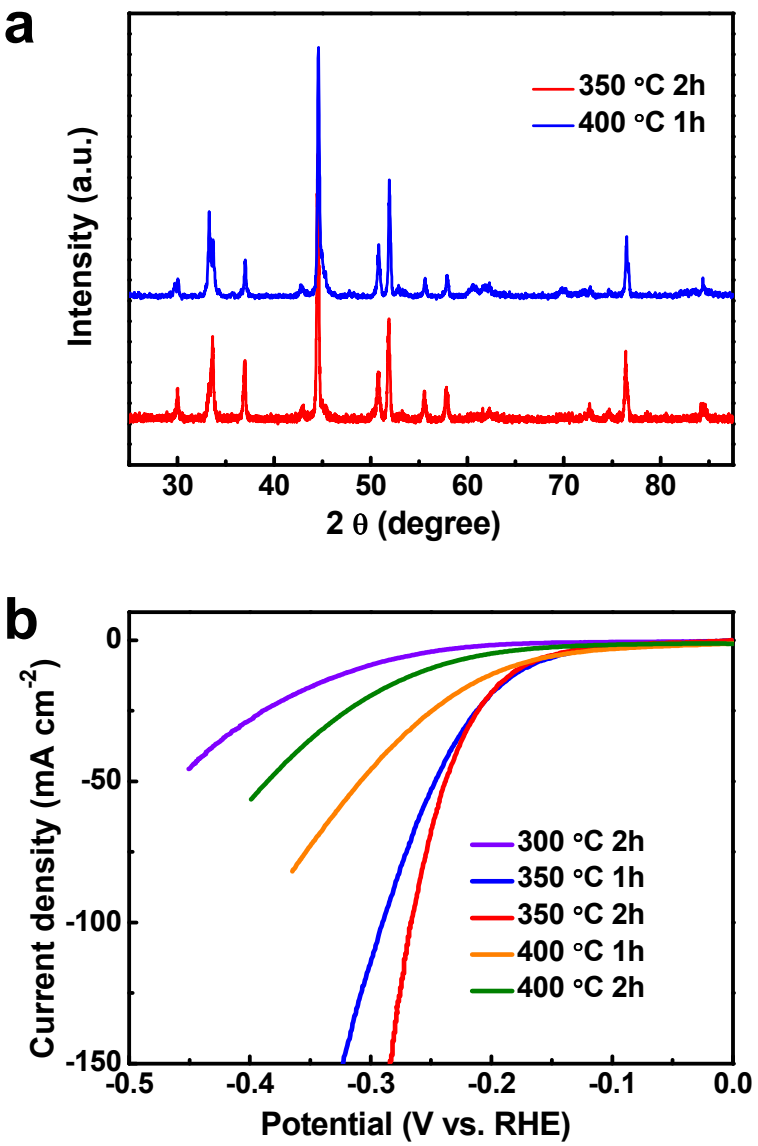


Figure S5. (a) XRD patterns and (b) polarization curves of $NiSe_2$/Ni obtained at different sintering temperatures and times.

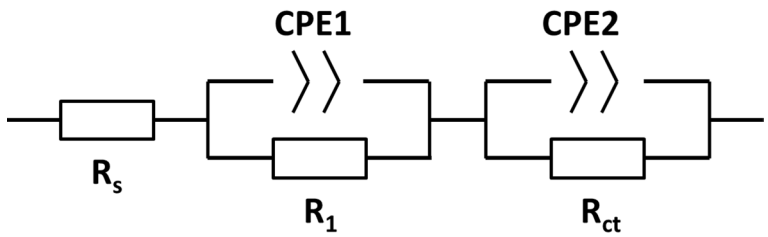


Figure S6. The equivalent circuit model used to fit the Nyquist plots of $NiSe_2$ shown in Figure 3(d) and 4(c).

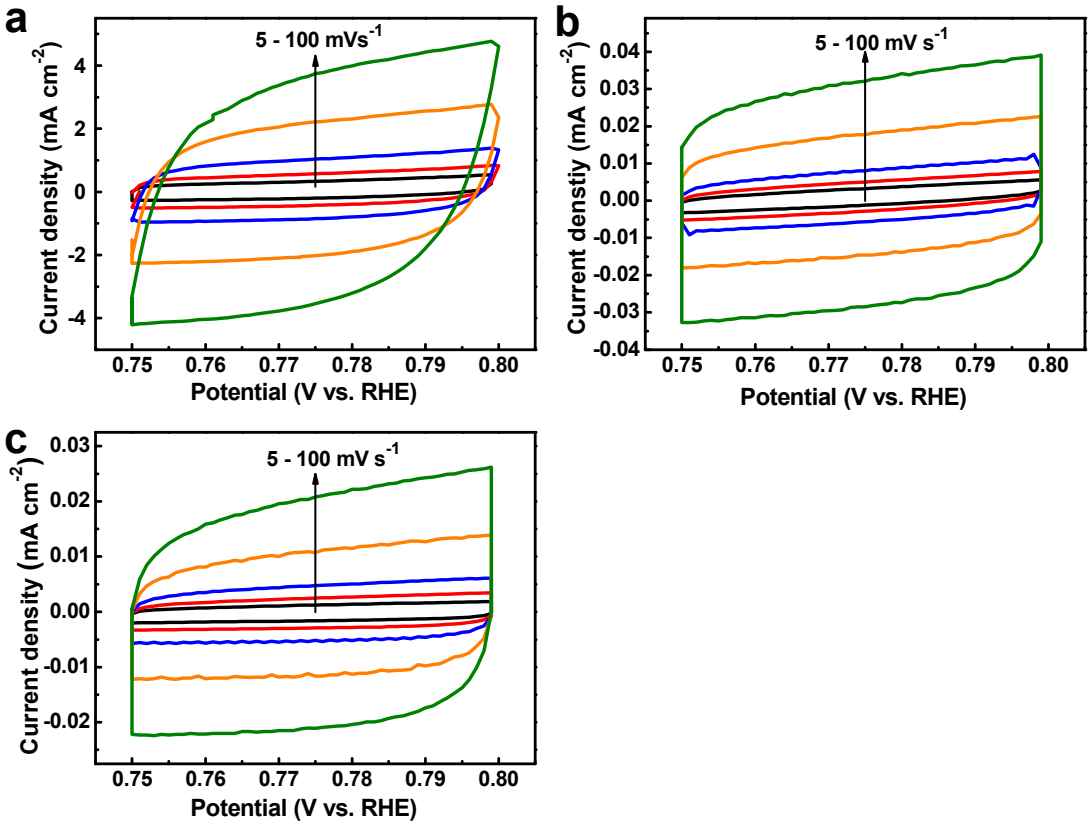


Figure S7. Cyclic voltammograms (CVs) for (a) $NiSe_2$/Ni, (b) $NiC_2O_4$/Ni, and (c) Ni foam measured in 1.0 M KOH at different scan rates from 5 to 100 mV $s^{-1}$.

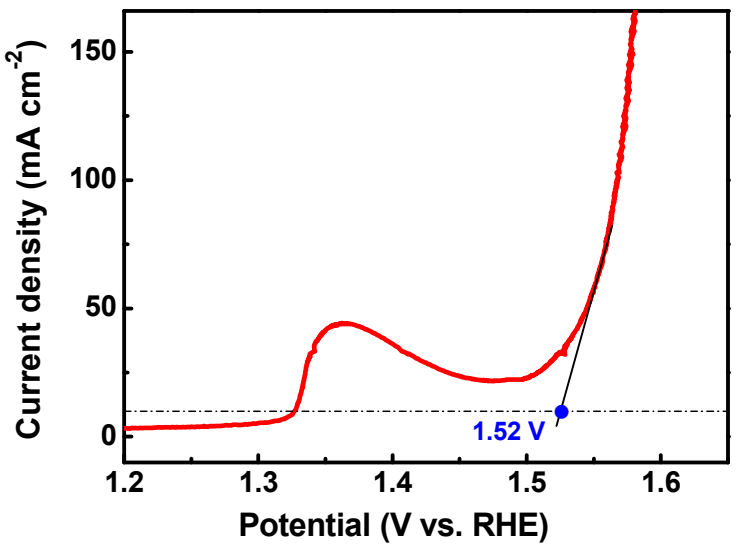


Figure S8. Polarization curves of $NiSe_2$/Ni electrode in 1.0 M KOH for OER at a scan rate of 5 mV $s^{-1}$.

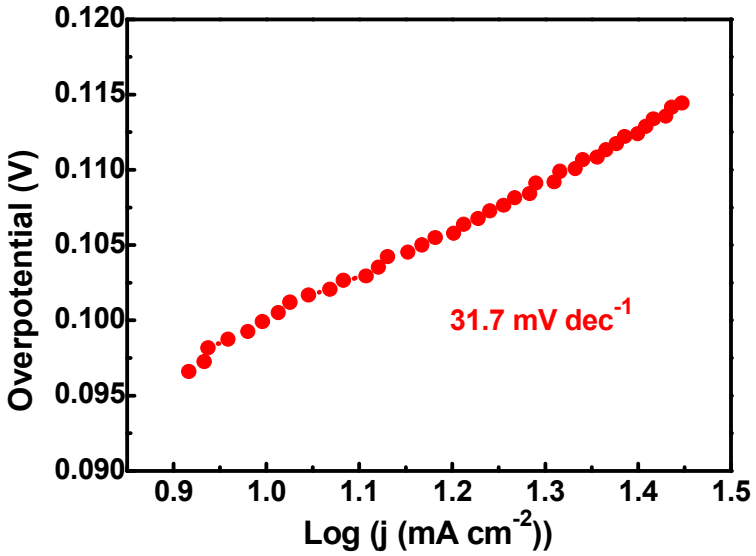


Figure S9. Tafel plot of $NiSe_2$/Ni for the oxidation process and/or adsorption of oxygenated species on $NiSe_2$.

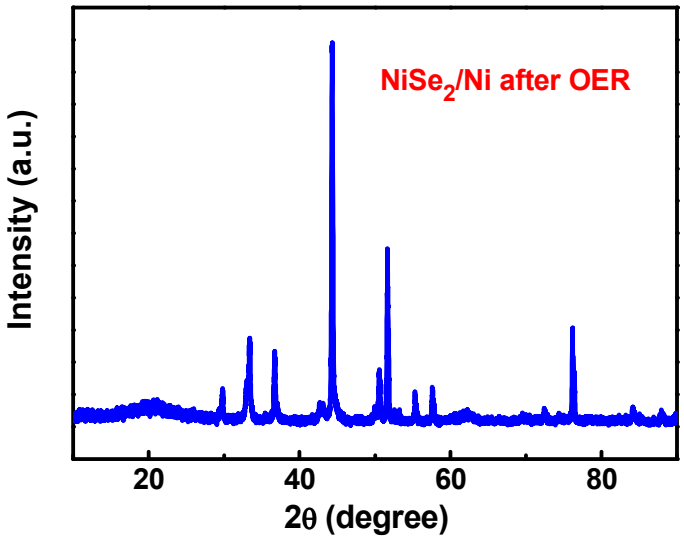


Figure S10. XRD pattern of $NiSe_2$/Ni after OER.

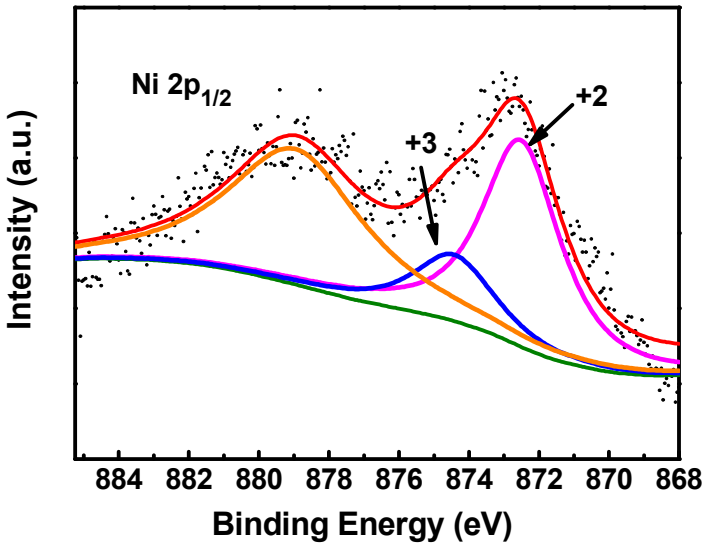


Figure S11. XPS spectrum of Ni $2p_{1/2}$ for the $NiSe_2$/Ni after the OER test.

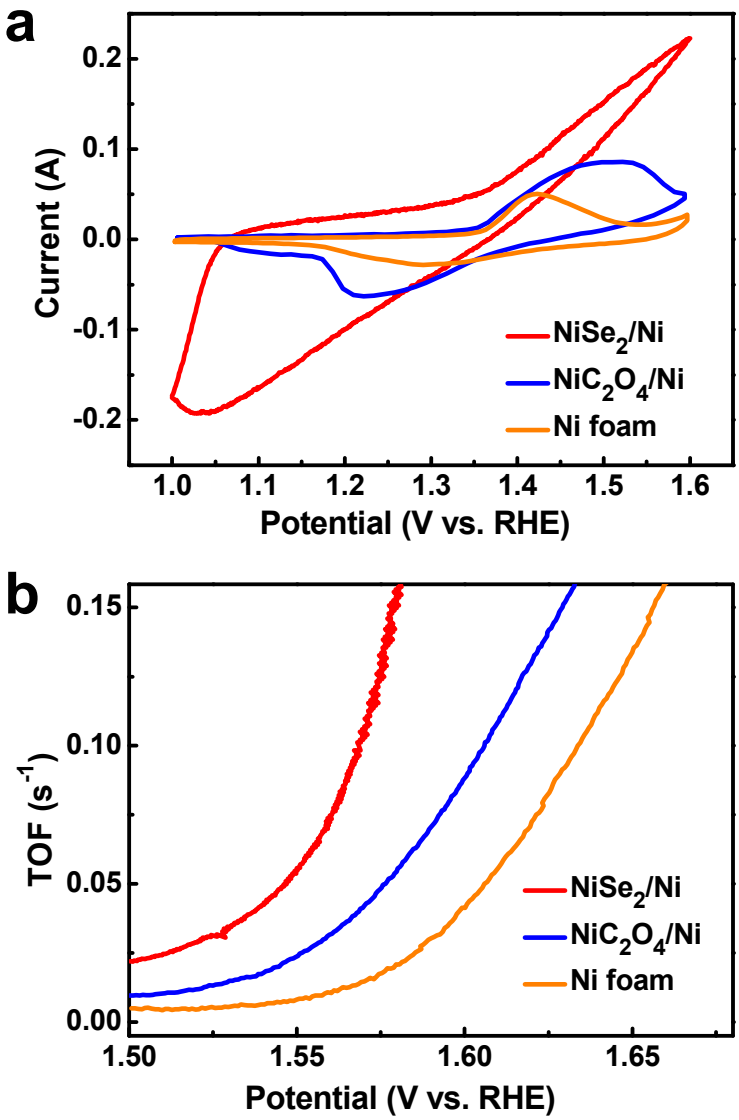


Figure S12. (a) CVs of different catalytic electrodes with the scan rate of 50 mV $s^{-1}$ in 1.0 M KOH and (b) Computed turnover frequency curves of different catalytic electrodes under OER conditions.

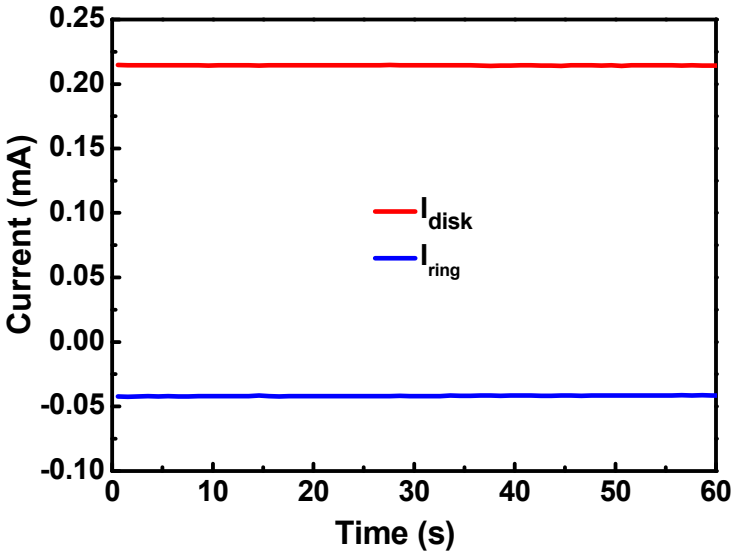


Figure S13. Ring and disk current of $NiSe_2$/Ni on an RRDE (1500 rpm) in $N_2$-saturated 0.1 M KOH solution (ring potential: 0.40 V vs. RHE).

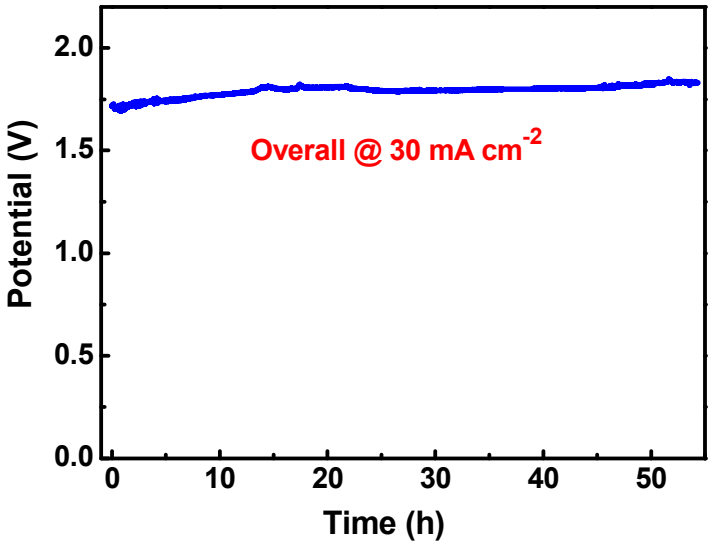


Figure S14. Long-term stability measurement of the $NiSe_2$/Ni-based electrolyzer at 30 mA $cm^{-2}$.

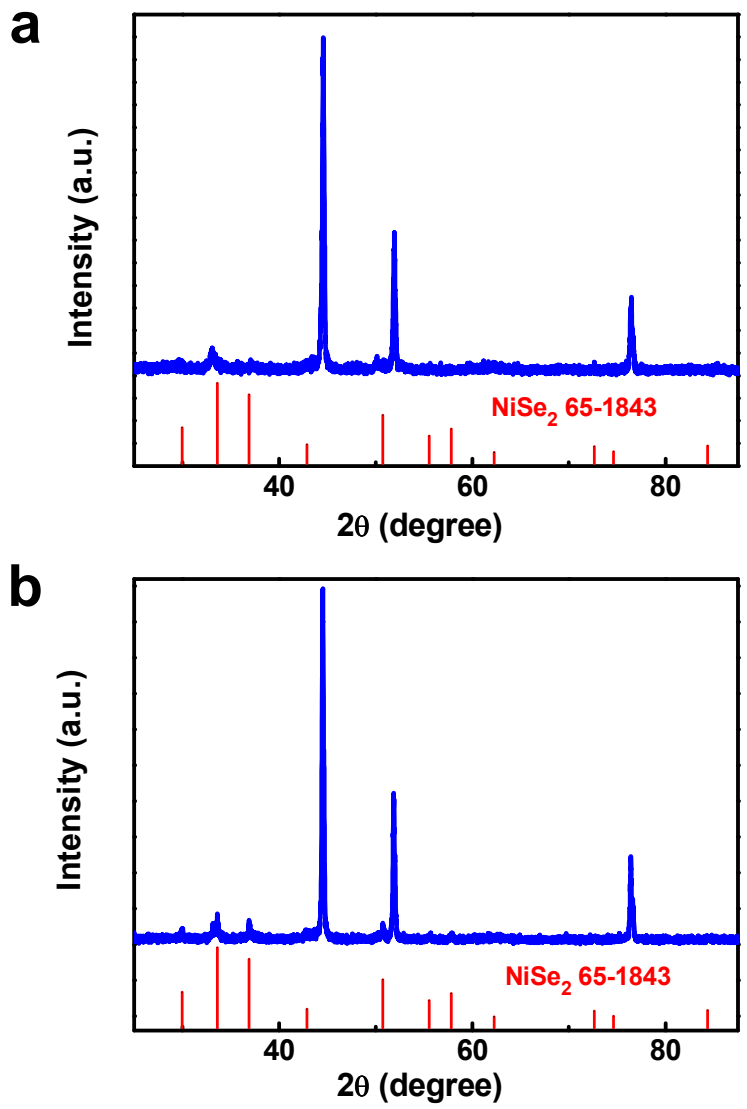


Figure S15. XRD patterns for $NiSe_2$ after the 80 h stability measurement of overall water splitting. (a) Cathode (HER) and (b) anode (OER).

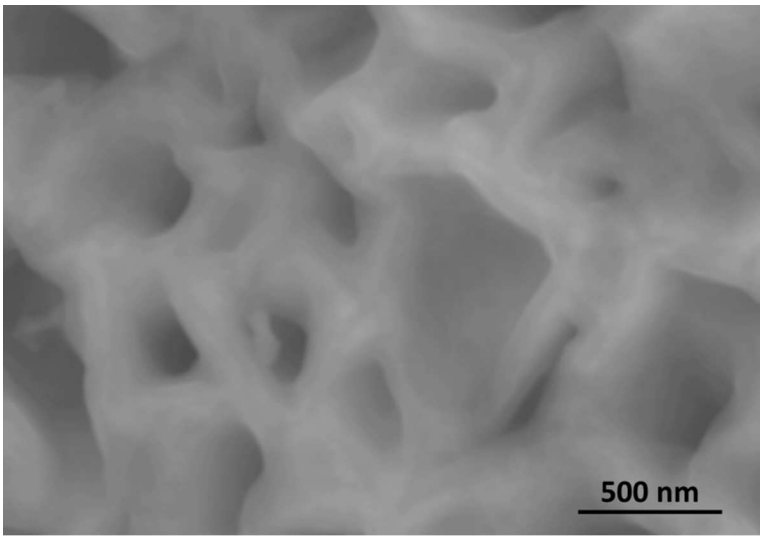


Figure S16. SEM image of the anode (OER) after the 80 h stability measurement of overall water splitting.

Table S1. Summary of recently reported HER electrocatalysts in 1.0 M KOH.

| **Catalysts** | **$\eta_0$ (mV)** | **$\eta_{10}$ (mV)** | **Tafel slope (mV dec$^{-1}$)** | **Reference** |
|---|---|---|---|---|
| Ni/NiS | ---- | 230 | 123 | S1 |
| CoP/CC | 115 | 209 | 129 | S2 |
| FeP NAs/CC | 86 | 218 | 146 | S3 |
| $Ni_{0.5}Co_{0.5}$ | ---- | 282 | 189 | S4 |
| $Ni_3S_2$/MWCNTs | ---- | 210 | 167 | S5 |
| Co@NRCNT | 160 | 370 | ---- | S6 |
| NiO/Ni-CNT | 90 | ~100 | 82 | S7 |
| Co@N-C | 130 | 210 | 108 | S8 |
| $Ni_2P$ | 100 | 240 | 87 | S9 |
| MoB | 120 | 230 | 59 | S10 |
| $Mo_2C$ | 100 | 190 | 54 | S10 |
| Fe-CoP/CC | ---- | 175 | 132 | S11 |
| DR-$MoS_2$ NW | ---- | 95 | 78 | S12 |
| **$NiSe_2$/Ni** | **56** | **166** | **92** | **Our work** |

Table S2. The mass density (loading) of $NiSe_2$ in the $NiSe_2$/Ni electrodes obtained at different sintering parameters.

| **Sintering parameter** | **Mass density (mg cm$^{-2}$)** |
|---|---|
| 300 °C 2h | 0.07 |
| 350 °C 1h | 2.1 |
| 350 °C 2h | 2.6 |
| 400 °C 1h | 3.2 |
| 400 °C 2h | 4.3 |

Table S3. Summary of exchange current density ($j_0$) for TMDs-based catalysts.

| **Catalysts** | ***$J_0$*** (mA $cm^{-2}$) | **Reference** |
|---|---|---|
| $CoSe_2$/CP | ~$(4.9 \pm 1.4)\times10^{-3}$ | S13 |
| Co/$CoSe_2$ | 0.033 | S14 |
| $CoSe_2$ | $5.7\times10^{-2}$ | S15 |
| $NiSe_2$ | $2.0\times10^{-3}$ | S15 |
| **$NiSe_2$/Ni** | **0.11** | **Our work** |

Table S4. Summary of recently reported OER electrocatalysts in 1.0 M KOH.

| **catalysts** | **$\eta_{10}$ (mV)** | **Reference** |
|---|---|---|
| $Ni_{0.33}Co_{0.67}S_2$ nanowires | 320 | S16 |
| $Ni_5P_4$ film | 290 | S17 |
| $NiFeO_x$ | 350 | S18 |
| NiCo LDH | 367 | S19 |
| $Ni_2P$ | 290 | S20 |
| $Ni(OH)_2$ | 330 | S21 |
| CoO/NG | 340 | S22 |
| NiO@Ni-Bi/CC | 290 | S23 |
| $Co_2N$/TM | 290 | S24 |
| $\alpha$-$Mn_2O_3$ | 340 | S25 |
| **$NiSe_2$/Ni** | **238** | **Our work** |

## References


[1] Chen, G.-F.; Ma, T. Y.; Liu, Z.-Q.; Li, N.; Su, Y.-Z.; Davey, K.; Qiao, S.-Z. Efficient and Stable Bifunctional Electrocatalysts Ni/NixMy(M = P, S) for Overall Water Splitting. *Adv. Funct. Mater.* **2016**, *26*, 3314-3323. http://doi.org/10.1002/adfm.201505626

[2] Tian, J.; Liu, Q.; Asiri, A. M.; Sun, X. Self-supported nanoporous cobalt phosphide nanowire arrays: an efficient 3D hydrogen-evolving cathode over the wide range of pH 0-14. *J. Am. Chem. Soc.* **2014**, *136*, 7587-7590. http://doi.org/10.1021/ja503372r

[3] Liang, Y.; Liu, Q.; Asiri, A. M.; Sun, X.; Luo, Y. Self-Supported FeP Nanorod Arrays: A Cost-Effective 3D Hydrogen Evolution Cathode with High Catalytic Activity. *ACS Catal.* **2014**, *4*, 4065-4069. http://doi.org/10.1021/cs501106g

[4] Bayatsarmadi, B.; Zheng, Y.; Russo, V.; Ge, L.; Casari, C. S.; Qiao, S. Z. Highly active nickel-cobalt/nanocarbon thin films as efficient water splitting electrodes. *Nanoscale* **2016**, *8*, 18507-18515. http://doi.org/10.1039/c6nr06961d

[5] Lin, T.-W.; Liu, C.-J.; Dai, C.-S. $Ni_3S_2$/carbon nanotube nanocomposite as electrode material for hydrogen evolution reaction in alkaline electrolyte and enzyme-free glucose detection. *Appl. Catal. B: Environ.* **2014**, *154-155*, 213-220. http://doi.org/10.1016/j.apcatb.2014.02.017

[6] Zou, X.; Huang, X.; Goswami, A.; Silva, R.; Sathe, B. R.; Mikmekova, E.; Asefa, T. Cobalt-embedded nitrogen-rich carbon nanotubes efficiently catalyze hydrogen evolution reaction at all pH values. *Angew. Chem. Int. Ed.* **2014**, *53*, 4372-4376. http://doi.org/10.1002/anie.201311111

[7] Gong, M.; Zhou, W.; Tsai, M. C.; Zhou, J.; Guan, M.; Lin, M. C.; Zhang, B.; Hu, Y.; Wang, D. Y.; Yang, J.; Pennycook, S. J.; Hwang, B. J.; Dai, H. Nanoscale nickel oxide/nickel heterostructures for active hydrogen evolution electrocatalysis. *Nat. Commun.* **2014**, *5*, 4695. http://doi.org/10.1038/ncomms5695

[8] Wang, J.; Gao, D.; Wang, G.; Miao, S.; Wu, H.; Li, J.; Bao, X. Cobalt nanoparticles encapsulated in nitrogen-doped carbon as a bifunctional catalyst for water electrolysis. *J. Mater. Chem. A* **2014**, *2*, 20067-20074. http://doi.org/10.1039/c4ta04337e

[9] Feng, L.; Vrubel, H.; Bensimon, M.; Hu, X. Easily-prepared dinickel phosphide ($Ni_2P$) nanoparticles as an efficient and robust electrocatalyst for hydrogen evolution. *Phys. Chem. Chem. Phys.* **2014**, *16*, 5917-5921. http://doi.org/10.1039/c4cp00482e

[10] Vrubel, H.; Hu, X. Molybdenum boride and carbide catalyze hydrogen evolution in both acidic and basic solutions. *Angew. Chem. Int. Ed.* **2012**, *51*, 12703-12706. http://doi.org/10.1002/anie.201207111

[11] Ma, M.; Zhu, G.; Xie, F.; Qu, F.; Liu, Z.; Du, G.; Asiri, A. M.; Yao, Y.; Sun, X. Homologous Catalysts Based on Fe-Doped CoP Nanoarrays for High

Performance Full Water Splitting under Benign Conditions. *ChemSusChem* **2017**, *10*, 3188-3192.
http://doi.org/10.1002/cssc.201700693

[12] Xie, J.; Qu, H.; Xin, J.; Zhang, X.; Cui, G.; Zhang, X.; Bao, J.; Tang, B.; Xie, Y. Defect-rich $MoS_2$ nanowall catalyst for efficient hydrogen evolution reaction. *Nano Res.* **2017**, *10*, 1178-1188.
http://doi.org/10.1007/s12274-017-1421-x

[13] Kong, D.; Wang, H.; Lu, Z.; Cui, Y. $CoSe_2$ nanoparticles grown on carbon fiber paper: an efficient and stable electrocatalyst for hydrogen evolution reaction. *J. Am. Chem. Soc.* **2014**, *136*, 4897-4900.
http://doi.org/10.1021/ja501497n

[14] Li, K.; Zhang, J.; Wu, R.; Yu, Y.; Zhang, B. Anchoring CoO Domains on $CoSe_2$ Nanobelts as Bifunctional Electrocatalysts for Overall Water Splitting in Neutral Media. *Adv. Sci.* **2016**, *3*, 1500426.
http://doi.org/10.1002/advs.201500426

[15] Kwak, I. H.; Im, H. S.; Jang, D. M.; Kim, Y. W.; Park, K.; Lim, Y. R.; Cha, E. H.; Park, J. CoSe(2) and NiSe(2) Nanocrystals as Superior Bifunctional Catalysts for Electrochemical and Photoelectrochemical Water Splitting. *ACS Appl. Mater. Interfaces* **2016**, *8*, 5327-5334.
http://doi.org/10.1021/acsami.5b12093

[16] Peng, Z.; Jia, D.; Al-Enizi, A. M.; Elzatahry, A. A.; Zheng, G. From Water Oxidation to Reduction: Homologous Ni-Co Based Nanowires as Complementary Water Splitting Electrocatalysts. *Adv. Energy Mater.* **2015**, *5*, 1402031.

http://doi.org/10.1002/aenm.201402031

[17] Ledendecker, M.; Krick Calderon, S.; Papp, C.; Steinruck, H. P.; Antonietti, M.; Shalom, M. The synthesis of nanostructured $Ni_5P_4$ films and their use as a non-noble bifunctional electrocatalyst for full water splitting. *Angew. Chem. Int. Ed.* **2015**, *54*, 12361-12365.
http://doi.org/10.1002/anie.201502438

[18] McCrory, C. C.; Jung, S.; Peters, J. C.; Jaramillo, T. F. Benchmarking heterogeneous electrocatalysts for the oxygen evolution reaction. *J. Am. Chem. Soc.* **2013**, *135*, 16977-16987.
http://doi.org/10.1021/ja510442p

[19] Liang, H.; Meng, F.; Caban-Acevedo, M.; Li, L.; Forticaux, A.; Xiu, L.; Wang, Z.; Jin, S. Hydrothermal continuous flow synthesis and exfoliation of NiCo layered double hydroxide nanosheets for enhanced oxygen evolution catalysis. *Nano Lett.* **2015**, *15*, 1421-1427.
http://doi.org/10.1021/nl504872s

[20] Stern, L.-A.; Feng, L.; Song, F.; Hu, X. $Ni_2P$ as a Janus catalyst for water splitting: the oxygen evolution activity of $Ni_2P$ nanoparticles. *Energy Environ. Sci.* **2015**, *8*, 2347-2351.
http://doi.org/10.1039/c5ee01155h

[21] Gao, M.; Sheng, W.; Zhuang, Z.; Fang, Q.; Gu, S.; Jiang, J.; Yan, Y. Efficient water oxidation using nanostructured alpha-nickel-hydroxide as an electrocatalyst. *J. Am. Chem. Soc.* **2014**, *136*, 7077-7084.
http://doi.org/10.1021/ja502128j

[22] Mao, S.; Wen, Z.; Huang, T.; Hou, Y.; Chen, J. High-performance bi-functional electrocatalysts of 3D crumpled graphene–cobalt oxide nanohybrids for oxygen reduction and evolution reactions. *Energy Environ. Sci.* **2014**, *7*, 609-616. http://doi.org/10.1039/c3ee42696c

[23] Zhang, R.; Wang, Z.; Hao, S.; Ge, R.; Ren, X.; Qu, F.; Du, G.; Asiri, A. M.; Zheng, B.; Sun, X. Surface Amorphization: A Simple and Effective Strategy toward Boosting the Electrocatalytic Activity for Alkaline Water Oxidation. *ACS Sustain. Chem. Eng.* **2017**, *5*, 8518-8522. http://doi.org/10.1021/acssuschemeng.7b01952

[24] Zhang, L.; Xie, L.; Ma, M.; Qu, F.; Du, G.; Asiri, A. M.; Chen, L.; Sun, X., Co-based nanowire films as complementary hydrogen- and oxygen-evolving electrocatalysts in neutral electrolyte. *Catal. Sci. Technol.* **2017**, *7*, 2689-2694. http://doi.org/10.1039/c7cy00703e

[25] Kölbach, M.; Fiechter, S.; van de Krol, R.; Bogdanoff, P., Evaluation of electrodeposited α-$Mn_2O_3$ as a catalyst for the oxygen evolution reaction. *Catal. Today* **2017**, *290*, 2-9. http://doi.org/10.1016/j.cattod.2017.03.030